Erzincan Üniversitesi
Fen Bilimleri Enstitüsü Dergisi
2023, 16(3), 854-868
ISSN: 1307-9085, e-ISSN: 2149-4584
Araştırma Makalesi

Erzincan University
Journal of ScienceandTechnology
2023, 16(3), 854-868
DOI: 10.18185/erzifbed.1266388
ResearchArticle

Synthesis, Antibacterial Activity and Molecular Modelling of Benzyl Acetate Derivatives

Bilal UMAR [1] Yusuf HASSAN [1*] Abdulhamid AHMED [2] Suat SARI [3] Xavier SIWE-NOUNDOU [4]

[1]Department of Chemistry, Faculty of Natural and Applied Sciences, Umaru Musa Yar'adua University, Katsina, Nigeria.

[2]Department of Biology, Faculty of Natural and Applied Sciences, Umaru Musa Yar'adua University, Katsina, Nigeria.

[3]Department of Pharmaceutical Chemistry, Faculty of Pharmacy, Hacettepe University, Ankara, Turkiye.

[4]Department of Pharmaceutical Sciences, School of Pharmacy, Sefako Makgatho Health Sciences University, Pretoria, South Africa.

0000-0001-8382-3296, 0000-0001-6117-2357, 0000-0002-0153-8334, 0000-0002-8248-4218, 0000-0002-8667-8351

Received: 12/12/2022, **Revised**: 23/092023, **Accepted**: 05/10/2023**, Published**: 31/12/2023

Abstract

Benzyl alcohol derivatives are known for their antibacterial efficacy. In this work five known benzyl acetate derivatives were synthesized by the acetylation of their corresponding benzyl alcohol derivatives and their structures confirmed using ^{1}H, ^{13}C NMR and FTIR spectroscopic techniques. The synthesized compounds were tested for antibacterial activity against *Staphylococcus aureus* and *Shigella spp* using disc diffusion method. Also the activity of amoxicillin disc (0.5 g/L) was measured as a positive control. Furthermore, the drug-likeness as well as the interactions of the compounds against the active site of *E. coli* carbonic anhydrase which share >98% similarity to that of *S. spp* were studied using molecular modelling method. The antibacterial activity showed that all the five compounds **3a-e** inhibited the two organisms at 100 µg/ml compared to the positive control. The largest inhibition zones of *Staphylococcus aureus* and *Shigella spp* were found to be 16.5 mm and 17.5 mm for compound **3d** and **3e**, respectively. Molecular modelling predicted the compounds to be water soluble, highly absorbed through GI tract, not Pgp substrates and not CYP3A4 inhibitors. Molecular docking studies showed that the compounds showed affinity to *E. coli* carbonic anhydrase active site, blocking access to the Zn^{2+} cofactor.

Keywords: Antibacterial activity, benzyl acetate derivatives, molecular modeling, *Staphylococcus aureus*, *Shigella spp*.

*Corresponding Author: yusuf.hassan@umyu.edu.ng
Bilal UMAR, https://orcid.org/0000-0001-8382-3296
Yusuf HASSAN, https://orcid.org/0000-0001-6117-2357
Abdulhamid AHMED, https://orcid.org/0000-0002-0153-8334
Suat SARI, https://orcid.org/0000-0002-8248-4218
Xavier SIWE-NOUNDOU, https://orcid.org/0000-0002-8667-8351

Benzil Asetat Türevlerinin Sentezi, Antibakteriyel Aktivitesi ve Moleküler Modellenmesi

Öz

Benzil alkol türevleri, antibakteriyel etkinlikleriyle bilinir. Bu çalışmada, bilinen beş benzil asetat türevi, karşılık gelen benzil alkol türevlerinin asetilasyonu ile sentezlendi ve yapıları, ^{1}H, ^{13}C NMR ve FTIR spektroskopik teknikleri kullanılarak doğrulandı. Sentezlenen bileşikler, disk difüzyon yöntemi kullanılarak Staphylococcus aureus ve Shigella spp'ye karşı antibakteriyel aktivite açısından test edildi. Ayrıca amoksisilin diskinin aktivitesi (0.5 g/L) pozitif kontrol olarak ölçüldü. Ayrıca, S. spp'ninkine >98% benzerlik paylaşan *E. coli* karbonik anhidrazın aktif bölgesine karşı bileşiklerin ilaca benzerliği ve etkileşimleri moleküler modelleme yöntemi kullanılarak incelenmiştir. Antibakteriyel aktivite, beş bileşik **3a-e**'nin hepsinin, pozitif kontrole kıyasla iki organizmayı 100 µg/ml 'de inhibe ettiğini gösterdi. Staphylococcus aureus ve Shigella spp'nin en büyük inhibisyon bölgeleri, bileşik **3d** ve **3e** için sırasıyla 16.5 mm ve 17.5 mm olarak bulundu. Moleküler modelleme, bileşiklerin suda çözünür olduğunu, GI yolu yoluyla yüksek oranda emildiğini, Pgp substratları ve CYP3A4 inhibitörleri olmadığını tahmin etti. Moleküler yerleştirme çalışmaları, bileşiklerin *E. coli* karbonik anhidraz aktif bölgesine afinite göstererek Zn^{2+} kofaktörüne erişimi engellediğini gösterdi.

Anahtar Kelimeler: Antibakteriyel aktivite, benzil asetat türevleri, moleküler modelleme, *Staphylococcus aureus, Shigella spp.*

1. Introduction

Antibiotic resistance is increasingly becoming a major public health problem globally [1]. The report on the review of antimicrobial resistance, commissioned by the UK government, highlights the global nature of the problem and recommends action on multiple measures to improve the production of new antibiotics [2]. Recently, a number of structurally diverse compounds were reported to have a wide range of antibacterial activities, these includes quinolinols [3], hydroxyquinolines, benzothiazoles [4], mercaptopropanoic acids [5], pyrazoles [6], and vanillyl alcohols [7]. However, the need for structurally simple compounds with promising activities and good pharmacokinetics continues to be of high interest.

In continuation of our efforts on the exploration of simple molecules as potential antimicrobial agents [7,8], we attempted to investigate the impact of an ester functionality on the antibacterial activity of the benzyl alcohol derivatives studied earlier [7,8]. Our literature search revealed that no biological activity of these esters has been reported. And since ester functionality appeared to be important in the structure of some essential medicines such as aspirin [9], clopidogrel [10], and statins [11]. It is thus conceived that the compounds designed in this study could potentially inhibit bacterial carbonic anhydrase (a new target for antibacterial compounds) because of their structural similarity to some compounds reported to demonstrate carbonic anhydrase inhibition (Figure 1) [12-14].

C. neoformans CA K_i = 0.0095 mM hCA II K_i = 4.8 mM

Figure 1. Compounds with CA Inhibitory Effects

Thus, five known benzyl acetate derivatives were synthesized and evaluated *in vitro* for their antibacterial activity against two bacterial species. The compounds were predicted to be druglike, have balanced pharmacokinetic features, and possibly show activity through bacterial carbonic anhydrase (CA) inhibition through molecular modelling studies.

2. Material and Methods

2.1. General

All chemicals were purchased from Sigma-Aldrich and used as received. ^{1}H and ^{13}C NMR spectra were recorded on a Bruker AVANCE 400 spectrometer. The FTIR spectra were recorded on Perkin–Elmer BX spectrophotometer.

2.2. Chemistry

2.2.1. General Procedure for the Preparation of Benzyl alcohols, 2a-e

Aldehyde (2g, 13.3 mmol) was transferred into an ice-bath cooled round bottom flask and dissolved in ethanol (4 ml). Then $NaBH_4$ (0.5g, 13.2 mmol) dissolved in 1M NaOH (3.8 ml) was added slowly to the aldehyde over a period of 10 minutes. The resulting mixture was stirred at room temperature for 10 minutes, and then cooled on an ice-bath. While stirring, 6M HCl was added dropwise until the evolution of H_2 gas stopped. The acidity of the mixture was measured using a pH meter and further stirred 10 minutes. The alcohol product was collected by filtration, washed twice with ice-cold water and air-dried. However, in the case of 3-nitrobenzaldehyde and 4-methoxybenzaldehyde, the corresponding alcohols were obtained by extracting the reaction mixture with chloroform and the solvent evaporated to furnish the appropriate alcohols. All compounds are known and their identities were confirmed by comparing their spectral data with those available in the literature [7,8,15,16].

4-hydroxy-3-methoxybenzyl alcohol, **2a**

White powder, 93% yield, mp 112-114˚C. ^{1}HNMR (400MHz,$DMSO_4$-d_6) δ ppm 3.74 (3H, s, OCH_3), 4.37 (2H, s, CH_2), 5.14 (1H, s, OH), 6.70 (2H, s, 2×Ar-H), 6.88 (1H, s, Ar-H), 8.88 (1H, s, ArOH); ^{13}CNMR (100MHz, $DMSO_4$-d_6) δ ppm 55.80 (OCH_3), 63.36 (CH_2), 111.32 (Ar-C), 115.35 (Ar-CH), 119.51 (Ar-CH), 133.72 (Ar- CH), 145.54 (ArC-OCH_3), 147.67 (Ar-COH); FTIR cm^{-1} 1121 (C-O), 3503 (OH).

3-nitrobenzyl alcohol, **2b**

Brown oil, 93% yield, ^{1}HNMR (400MHz, $DMSO_4$-d_6) δ ppm 3.56 (2H, s, CH_2), 5.61 (1H, s, OH), 7.37 (1H, t, *J* = 8.0 Hz, Ar-H), 7.57 (2H, d, *J* = 8.0 Hz, Ar-H), 8.17 (2H, d, *J* = 4.0 Hz, Ar-H); ^{13}C NMR (100MHz, $DMSO_4$-d_6) δ ppm62.21 (CH_2), 123.49 (ArCH), 125.49 (ArCH), 127.25 (ArCH), 130.12 (ArCH), 148.50(Ar-C), 150.89 (Ar-CNO_2); FTIR cm^{-1} 1230 (C-O), 3506 (OH).

4-hydroxybenzyl alcohol, **2c**

White powder, 87% yield, mp 260-265 ˚C; ^{1}HNMR (400MHz,$DMSO_4$-d_6) δ ppm 4.37 (2H, s, CH_2), 5.07 (1H, s, OH), 6.71 (2H, d, *J* = 8.0 Hz, Ar-H), 7.11 (2H, d, *J* = 8.0 Hz, Ar-H), 9.36 (1H, s, Ar-OH); ^{13}CNMR (100MHz, $DMSO_4$-d_6) δ ppm 63.09 (CH_2), 115.10 (2×ArCH), 128.43 (2×ArCH), 132.94 (Ar-C), 156.41 (Ar-COH); FTIR cm^{-1} 1207 (C-O), 3377 (OH).

4-methoxybenzyl alcohol, **2d**

Yellow oil; 94% yield; mp 212-215 ˚C; ^{1}HNMR (400MHz, $DMSO_4$-d_6) δ ppm 3.71 (3H, s, OCH_3), 4.40 (2H, s, CH_2), 5.15 (1H, s, OH), 6.87 (2H, d, *J* = 8.0 Hz, Ar-H), 7.22 (2H, d, *J* = 8.0 Hz, Ar-H); ^{13}CNMR (100MHz, $DMSO_4$-d_6) δ ppm 55.22 (OCH_3), 62.79 (CH_2), 113.67 (Ar-C), 128.21 (2×ArCH), 128.82 (2×ArCH), 158.36 (Ar-$COCH_3$), FTIR cm^{-1} 1244 (C-O), 3326 (OH).

4-chlorobenzyl alcohol, **2e**

White powder; 95% yield; mp 212-215 ˚C; 1H NMR (400MHz, $DMSO_4$-d_6) δ ppm 4.46 (2H, s, CH_2), 5.38 (1H, s, OH), 7.27 (2H, d, *J* = 8.0 Hz, Ar-H), 7.48 (2H, d, *J* = 8.0 Hz, Ar-H); ^{13}C NMR (100MHz, $DMSO_4$-d_6) δ ppm 62.40 (CH_2), 119.81 (Ar-C), 128.79 (2×ArCH), 131.12 (2×ArCH), 142.06 (Ar-CCl); FTIR cm^{-1} 1203 (C-O), 3290 (OH).

2.2.2. General Procedure for the Preparation of Benzyl acetates, 3a-e

A 5 ml reaction bottle was charged with benzyl alcohol (1 mmol) and acetic anhydride (1.5 mmol) and thoroughly mixed. The reaction bottle was placed on a pre-heated water bath (60˚C) for the required time. After completion of the reaction as monitored by TLC, the reaction mixture was treated with diethyl ether.

The ether solution was washed with sodium bicarbonate (10 ml × 2) and the solvent evaporated to afford the ester products. The identity of the compounds was confirmed by comparing their spectral data with the literature [17].

4-hydroxy-3-methoxybenzyl acetate, **3a**

Yellow oil, 94% yield. ^{1}H NMR (400 MHz, $CDCl_3$) δ 2.09 (s, 3H, CH_3), 2.30 (s, 3H, OCH_3), 3.83 (s, 2H, CH_2), 5.06 (s, 1H, OH), 7.02-6.87 (m, 3H, Ar-H).^{13}C NMR (100 MHz, $CDCl_3$) δ 20.68 (CH_3), 55.96 (OCH_3), 66.01 (CH_2), 112.62 (Ar-C), 120.80 (Ar-C), 122.89 (Ar-C), 134.89 (Ar-C), 139.75 (Ar-C), 151.19 (Ar-C), 169.04 (C=O). FTIR cm^{-1}1192 (C-O), 1736 (C=O), 3444 (OH).

3-nitrobenzyl acetate, **3b**

Yellow oil, 95% yield. ^{1}H NMR (400 MHz, $CDCl_3$) δ 2.14 (s, 3H, CH_3),5.19 (s, 2H, CH_2), 7.55 (t, *J* = 7.9 Hz, 1H, Ar-H), 7.68 (d, *J* = 7.7 Hz, 1H, Ar-H), 8.18 (d, *J* = 8.2 Hz, 1H, Ar-H), 8.22 (s, 1H, Ar-H). ^{13}C NMR (100 MHz, $CDCl_3$) δ 20.97 (CH_3), 64.92 (CH_2), 122.95 (Ar-C), 123.26 (Ar-C), 129.70 (Ar-C), 134.03(Ar-C), 138.20 (Ar-C), 148.50 (Ar-C), 170.70 (C=O). FTIR cm^{-1} 1222 (C-O), 1736 (C=O).

4-hydroxybenzyl acetate, **3c**

Yellow oil, 94% yield. ^{1}H NMR (400 MHz, $CDCl_3$) δ 2.17 (s, 3H, CH_3), 4.96 (s, 2H, CH_2), 6.95 (d, *J* = 8.6 Hz, 2H, Ar-H), 7.13 (s, 1H, OH), 7.24 (d, *J* = 8.4 Hz, 2H, Ar-H).^{13}C NMR (100 MHz, $CDCl_3$) δ 21.26 (CH_3), 65.78 (CH_2), 121.87 (2×Ar-C), 129.68 (2×Ar-C), 130.45 (Ar-C), 150.67 (Ar-C), 169.60 (C=O). FTIR cm^{-1}1132 (C-O), 1707 (C=O), 3034 (OH).

4-methoxybenzyl acetate,**3d**

Yellow oil, 97% yield. ^{1}H NMR (400 MHz, $CDCl_3$) δ 2.03(s, 3H, CH_3), 4.42(s, 3H, OCH_3), 5.00 (s, 2H, CH_2), 7.26-7.23 (m, 4H, Ar-H). ^{13}C NMR (100 MHz, $CDCl_3$) δ 21.05 (CH_3), 66.12 (CH_2), 71.48 (OCH_3), 113.97 (Ar-C), 129.43 (Ar-C), 131.99 (Ar-C), 164.64 (Ar-C), 170.98 (C=O).FTIR cm^{-1}1237 (C-O), 1736 (C=O).

4-chlorobenzyl acetate, **3e**

Yellow oil, 98% yield ^{1}H NMR (400 MHz, $CDCl_3$) δ 2.06 (s, 3H, CH_3), 5.03 (s, 2H, CH_2), 7.31-7.22 (m, 4H, Ar-H). ^{13}C NMR (100 MHz, $CDCl_3$) δ 21.09 (CH_3), 65.59 (CH_2), 128.88 (2×Ar-C), 129.77 (2×Ar-C), 134.28 (Ar-C), 134.57 (Ar-C), 170.92 (C=O). FTIR cm^{-1}1222 (C-O), 1736 (C=O).

2.3. Antibacterial Assay

The antibacterial assay was conducted against the two bacterial species, *Staphylococcus aureus* and *Shigella spp* following the standard method reported in our earlier works [7,8].

2.4. Data Analysis

The data were analyzed using MS Excel 2007 and expressed as mean ± SD of three replicates. The statistical difference of the mean zone of inhibition of the compounds for individual bacteria was carried out by employing one-way analysis of variance (ANOVA) followed by Tukey's post hoc multiple comparison test using the 'Statistical Package for Social Sciences (version 20.0) software' at a significance level of $p<0.05$.

2.5. Molecular Modelling

Legends were prepared, modelled, and optimized using LigPrep(2021-4, Schrödinger LLC, New York, NY)and Macro Mode(2021-4, Schrödinger LLC, New York, NY)according to the OPLS4 (2021-4, Schrödinger LLC, New York, NY)force field parameters [18] and conjugate gradient algorithm. Molecular descriptors were calculated using Swiss ADME (www.swissadme.ch) [19] and the target prediction was performed using Swiss Target Prediction (www.swisstargetprediction.ch) [20]. BLAST search was performed NCBI BLAST web tool (https://blast.ncbi.nlm.nih.gov) [21]. Crystallographic structure of *Escherichia coli* CA (PDB code: 1I6O, resolution: 2.20 Å) [22] was downloaded from the RCSB Protein Data Bank and prepared for docking using the Protein Preparation Wizard of Maestro(2021-4, Schrödinger LLC, New York, NY) [23]. During this process redundant molecules were removed, hydrogen atoms were added, partial charges and bond orders were assigned, ionization and tautomeric states of certain residues were generated, water molecules were sampled, H bonds were assigned and restrained minimization was performed (convergence cut-off for heavy atoms: 0.3 Å). The active site cavity for docking was defined as a cube of 27.000$Å^3$ centering on the Zn^{2+} co-factor (central coordinates: 44.15, -6.65, and 63.53). Molecular docking was performed with Glide (2021-4, Schrödinger LLC, New York, NY) at extra precision at 100 runs per ligand following generation of the active site grids [24]. Five ligand-receptor complexes of each compounds **3a-e** with the best docking score were selected and subject to MM-GBSA calculations to calculate free energy of binding (ΔG) using Prime (2021-4, Schrödinger LLC, New York, NY) [25]. In these calculations, VGSB solvation model and OPLS4 force field parameters were used, amino acid residues within 5 Å of ligand were kept flexible, and the resulting complexes were sampled according to force field minimization.

3. Results and Discussion

3.1. Chemistry

The synthesis of the benzyl acetate derivatives **3a-e** was achieved by the acetylation of the corresponding benzyl alcohols which were obtained by the $NaBH_4$ reduction of the corresponding benzaldehydes (Scheme 1). The compounds were characterized using ^1H and ^{13}C NMR, as well as FTIR spectroscopic techniques.

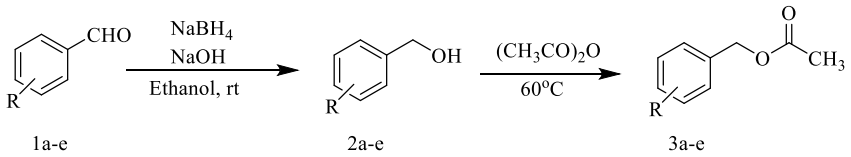

a	4-OH, 3-OCH_3
b	3-NO_2
c	4-OH
d	4-OCH_3
e	4-Cl

Scheme 1. Synthesis of Benzyl acetate Derivatives

3.2. Antibacterial Activity

Compounds **3a-e** were screened for *in vitro* antibacterial activity against Gram-positive and negative bacteria, *Staphylococcus aureus* and *Shigella species*, respectively (Table 1).

Table 1. Zone of Inhibition (mm)[a]

		Concentration (μg/ml)			
Compound	Organism	100	50	25	12.5
3a	*S. aureus*	9.5±0.5	9.0±0.0	0.0±0.0	0.0±0.0
	S. spp	12.5±0.5	9.0±0.5	0.0±0.0	0.0±0.0
3b	*S. aureus*	11.0±0.0	9.5±0.5	0.0±0.0	0.0±0.0
	S. spp	8.0±0.0	7.0±0.0	7.0±0.0	0.0±0.0
3c	*S. aureus*	9.5±0.5	8.0±0.0	7.0±0.5	0.0±0.0
	S. spp	8.0±0.5	0.0±0.0	0.0±0.0	0.0±0.0
3d	*S. aureus*	16.5±0.5	9.0±0.0	7.0±0.0	7.0±0.0
	S. spp	13.5±0.5	8.0±0.0	0.0±0.0	0.0±0.0
3e	*S. aureus*	9.0±0.0	0.0±0.0	0.0±0.0	0.0±0.0
	S. spp	17.5±0.5	12.0±0.5	10.0±0.5	9.0±0.0

[a]Control = Amoxicillin Disc (0.5g/L): *S. aureus* = 42.0 mm; *Shigella spp* = 36 mm

Compound **3d** was found to be active (16.5±0.5 mm) against *Staphylococcus aureus* at 100 µg/ml followed by compound **3b** with mean of inhibition of 11.0±0.0 mm. At this concentration, compounds **3a** and **3c** were found to have the same activity of 9.5±0.5 mm mean of inhibition. *Staphylococcus aureus* was found to be slightly resistant to compound **3e** at 100 µg /ml with 9.0±0.0 mean of inhibition. At 50 µg/ml, all of the compounds were found to have similar zones of inhibition except compound **3e** which showed no inhibition.

Compounds **3a**, **3b** and **3d** gave 9.0±0.0 mm, 9.5±0.5 mm, and 9.0±0.0 mm means of inhibition respectively, while **3c** showed 8.0±0.0 mm mean zone of inhibition. At 25 µg/ml, compounds **3a**, **3b** and **3e** showed no inhibition against *Staphylococcus aureus*, whereas compounds **3c** and **3d** showed 7.0±0.5 mm and 7.0±0.0 mm mean of inhibition respectively. Similarly, at the lowest concentration (12.5 µg/ml), only compound **3d** showed zone of inhibition, 7.0±0.0. This result gave the highest activities for all the compounds at 100 µg /ml, especially compound **3d** which contains the methoxy substituent which implied the role of the electron donating effect of the methoxy group on the activity observed.

In the case of Gram-negative bacteria, *Shigella spp*, it was found that compound **3e** exhibited the highest zones of inhibition at 100 µg/ml with a mean zone of inhibition of 17.5±0.5 mm. This was followed by compounds **3a** and **3d** with mean zones of 12.5±0.5 mm and 13.5±0.5 mm respectively. At this concentration, compounds **3b** and **3c** were found to have 8.0±0.0 mm and 8.0±0.5 mm mean of inhibition respectively. This implied that, *Shigella spp* was slightly resistant to these two compounds. At 50 µg/ml, compound **3c** showed no inhibition, whereas other compounds showed promising activity especially compound **3e** with mean zone of 12.0±0.5 mm, followed by compound **3a, 3d** and lastly **3b** with mean zones of 9.0±0.5 mm, 8.0±0.0 mm and 7.0±0.0 mm respectively. At 25 µg/ml, only compounds **3b** and **3e** inhibited the growth of *Shigella spp* with mean of 7.0±0.0 mm and 10.0±0.0 mm respectively. Similarly, only compound **3e** showed inhibition of 8.0±0.5 mm at the lowest concentration of 12 µg/ml. Overall, the activities of compouds **3a-e** were found to be highest at 100 µg/ml with compound **3e** bearing the chloro group exhibiting the highest zone of inhibition. The chloro group as a ring deactivating group had apparently played a role in the activity observed in the case of *Shigella spp* unlike *Staphylococcus aureus* where the activity was due to an activating group.

3.3. Drug-like Chemical Space

It is important to predict drug-likeness, as well as certain physicochemical and pharmacokinetic parameters (Table 2) to avoid attritions in the later phases of drug design. Therefore, we calculated descriptors that are relevant to orally available drug-like chemical space, namely molecular weight (MW), number of rotatable bonds (RB), hydrogen bond acceptor and donor counts (HA and HD), molar refractivity (MR), total polar surface area (PSA), and logP, and evaluated the results according to the rule sets of Lipinski, Veberand Ghose [26-28]. In addition, some key physicochemical/pharmacokinetic properties such as aqueous solubility, gastrointestinal (GI) absorption, P-glycoprotein (Pgp) binding (being a Pgp substrate), and CYP3A4 inhibition were predicted. CYP3A4 is a common microsomal enzyme for xenobiotic metabolism and its inhibition leads to serious drug/food interactions [29]. Efflux pumps, such as Pgp, can reduce availability of their substrates in drug action sites and cause drug interactions

[30]. The drug-likeness criteria of all the title compounds were found to be acceptable. Since none of them were identified as pan-assay interference compounds (PAINS) [31]. Also the compounds were predicted to be water soluble, highly absorbed through GI tract, not Pgp substrates and not CYP3A4 inhibitors (Table 2).

Table 2. Physicochemical and pharmacokinetic parameters calculated for compound, **3a-e**

Compound	MW (Da)[a]	RB[b]	HA[c]	HD[d]	MR[e]	PSA (Å^2)[f]	LogP[g]	Sol.[h]	GI abs.	Pgp subs.	CYP3A4 inh.	PAINS
3a	196.2	4	4	1	50.8	55.8	1.3	Very soluble	High	No	No	No
3b	195.2	4	4	0	51.1	72.1	1.4	Soluble	High	No	No	No
3c	166.2	3	3	1	44.3	46.5	1.5	Soluble	High	No	No	No
3d	180.2	4	3	0	48.8	35.5	1.9	Soluble	High	No	No	No
3e	184.6	3	2	0	47.3	26.3	2.5	Soluble	High	No	No	No

[a]Ideal values: ≤ 500 (Lipinski), 160-480 (Ghose), [b]Ideal values: ≤ 500 (Veber), [c]Ideal values: ≤ 10 (Lipinski), [d]Ideal values: ≤ 5 (Lipinski), [e]Ideal values:40-130 (Ghose), and [f]Ideal values: ≤ 140 (Veber), [g] Consensus of the results from five different methods are presented. Ideal values: ≤ 5 (Lipinski), -0.4-5.6 (Ghose) and [h]Results from the ESOL method are provided.

3.4. Molecular Docking

In light of the drug-likeness of the compounds, we decided to perform the molecular docking of **3a-e** with *Escherichia coli* CA, a homodimer β-CA, which was followed by MM-GBSA calculations to obtain more precise ligand binding affinity. The choice of this enzyme was due to the unavailability of the crystallographic structure for *S. aureus* or *Shigella spp.* CA. Incidentally, however, the *E. coli* CA shows very high sequence identity (>98%) to *Shigella spp.* CA, whose structure was resolved via X ray crystallography [22]. Following the molecular docking study, it was found that, two carbonic anhydrase isoforms were among the top 10 protein targets predicted for compound **3e** (Table 3).

Table 3. Possible protein targets predicted for compound, **3e**

Target	Common name	Uniprot ID
Beta-chymotrypsin	CTRB1	P17538
Thymidylate synthase	TYMS	P04818
Acyl coenzyme A:cholesterol acyltransferase	CES1	P23141
Telomerase reverse transcriptase	TERT	O14746
Carboxylesterase 2	CES2	O00748
Leukocyte common antigen	PTPRC	P08575
Metabotropic glutamate receptor 5	GRM5	P41594
Huntingtin	HTT	P42858
Carbonic anhydrase II	CA2	P00918
Carbonic anhydrase I	CA1	P00915

The results further indicated that compound **3a-e** showed affinity to *E. coli* CA active site (Table 3), which is located at the dimer interface and accommodates a Zn^{2+} cofactor. Apart from a water molecule, Zn^{2+} coordinates with electron donors from two cysteine (Cys42 and Cys101), one aspartate (Asp44) and histidine (His98) residues. The molecular docking study suggested two distinct binding modes for the compounds. Although in neither mode the compounds engaged in direct contacts with the Zn^{2+}, in the case of **3b**, strong electrostatic interactions were predicted with Asp44, a Zn^{2+} ligand, and Arg46, a key residue contributing to the catalytic function of Asp44 [22], which are of the same chain (Figure 2).

In the alternative binding mode, as exemplified by **3d** and **3e**, the compounds predictably blocked access to the Zn^{2+} pocket by clinging to Tyr83 of the opposite chain (Figure 2). Tyr83 is believed to play pivotal role in proton transfer for the catalytic function of β-CAs [32,33]. In both binding modes, the compounds were predicted to fit in the cavity and engage with both chains of the interface (Figure 2).

Table 4. Docking scores (kcal/mol) and free ΔG (kcal/mol) of **3a-e** with *E. coli* CA

3	Docking score	ΔG
a	-4.5	-19.2
b	-2.7	-23.9
c	-3.8	-27.4
d	-3.3	-17.3
e	-3.2	-19.4

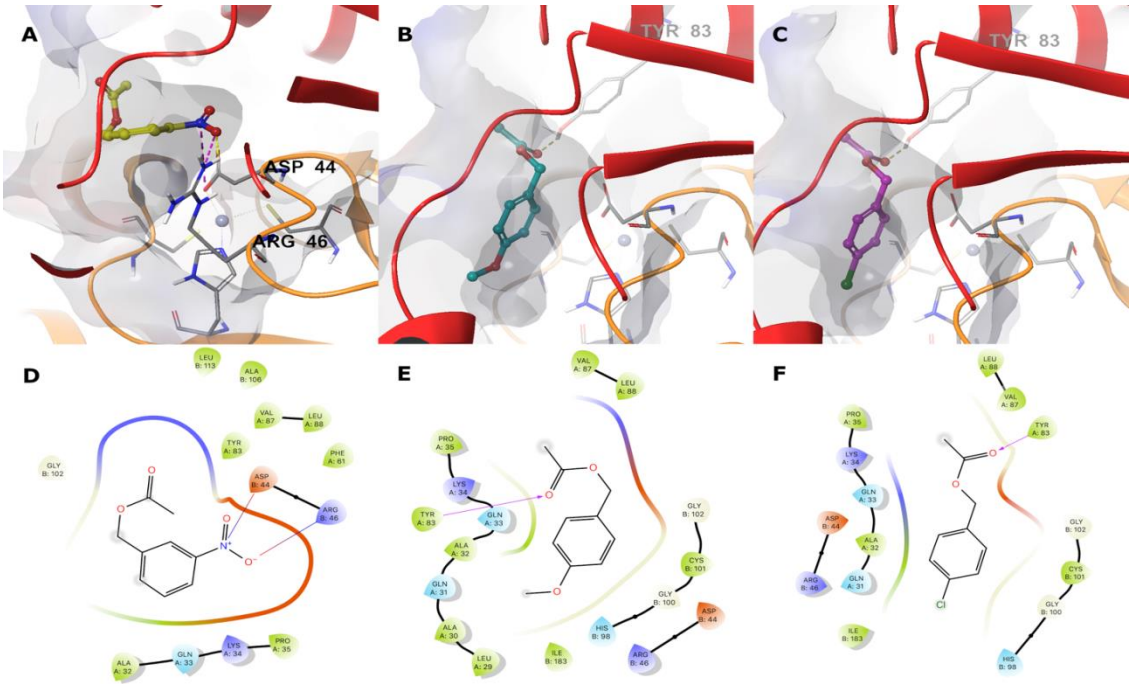

Figure 2. Predicted binding modes of compound**3b** (A), **3d** (B), and**3e** (C) in *E. coli* CA active site. Ligands are showed in color stick-ball representation, amino acid residues as gray sticks, Zn^{2+} as gray sphere, and protein backbone as color ribbons. Protein molecular surface is rendered, electrostatic interactions are indicated as dashed lines, and interacting residues are labeled. Complete predicted binding interactions for the compounds are provided as 2D interactions diagrams (D-F, respectively).

4. Conclusion

Synthesis of five known benzyl acetate derivatives was achieved and the compounds were evaluated *in vitro* for antibacterial activity against *Staphylococcus aureus* and *Shigella spp*.The zones of inhibition of the five compounds,**3a-e** revealed that the compounds were effective against the two organisms at 100µg/ml. Molecular modelling suggested that the title compounds were druglike, non-PAINS and had favorable pharmacokinetic profiles. Molecular modelling also suggested that the compounds most probably acted through bacterial CA inhibition through binding to the active site and blocking substrate access to the catalytic Zn^{2+}. Further studies are intended to verify CA inhibitory properties of the compounds and optimize them accordingly by rational structural modifications to improve their antibacterial efficacy.

Ethics in Publishing

There are no ethical issues regarding the publication of this study.

Author Contributions

Concept – Y. H., A. A.; Design – Y. H., A. A., S. S.; Supervision – Y. H., A. A.; Resources − B. U., Y. H., A. A., S. S., X. S.-N.; Materials – B. U., Y. H., A. A., S. S., X. S.-N.; Data Collection and/or Processing – B. U., S. S., X. S.-N.; Analysis and/or Interpretation – B. U., Y. H., A. A., S. S., X. S.-N.; Literature Search – B. U., Y. H., A. A., S. S.; Critical Reviews – Y. H., A. A., S. S., X. S.-N.

Acknowledgements

Mannir Kabir, Department of Microbiology, Umaru Musa Yar'adua University, Katsina, Nigeria is gratefully acknowledged for the antibacterial assay.

References

[1] MacGowan, A., Macnaughton, E. (2017). Antibiotic resistance. *Medicine*, 45(10), 622-628.

[2] Tackling Drug-Resistant Infections Globally: Final Report and Recommendations, Review on Antimicrobial Resistance.https://amrreview.org (accessed on April 2017).

[3] El Faydy, M., Dahaieh, N., Ounine, K., Lakhrissi, B., Warad, I., Tüzün, B., Zarrouk, A. (2021). Synthesis, Identification, Antibacterial Activity, ADME/T and 1BNA-Docking Investigations of 8-Quinolinol Analogs Bearing a Benzimidazole Moiety. *Arab. J. Sci. Eng*. 47(1), 497-510.

[4] Nehra, N., Tittal, R., K., Ghule, V. D. (2021). 1,2,3-Triazoles of 8-Hydroxyquinoline and HBT: Synthesis and Studies (DNA Binding, Antimicrobial, Molecular Docking, ADME, and DFT). *ACS Omega*, 6, 27089−27100.

[5] Salihovic, M., Pazaljaa, M., Halilovic, S. S., Veljovic, E., Mahmutovic-Dizdarevi, I., Roca, S., Novakovic, I., Trifunovic, S. (2021). Synthesis, characterization, antimicrobial activity and DFT study of some novel Schiff bases. *J. Mol. Struct*., 1241, 130670.

[6] Cetin, A., Bildirici, I. (2018). A study on synthesis and antimicrobial activity of 4-acyl-pyrazoles. *J. Saudi Chem. Soc.*, 22, 279–296.

[7] Sulaiman, M., Hassan, Y., Taskin-Tok, T., Siwe-Noundou, X. (2020). Synthesis, Antibacterial Activity And Docking Studies Of Benzyl Alcohol Derivatives. JOTCSA, 7(2), 481–8.

[8] Ogala, J. B., Hassan, Y., Samaila, A., Bindawa, M. I., Taskin-Tok, T. (2022). Synthesis, Antifungal Activity, and *In Silico* ADMET Studies of Benzyl alcohol Derivatives. *Istanbul J. Pharm.*, 52(1), 47-53.

[9] Romano, M., Cianci, E., Simiele, F., Recchiuti, A. (2015). Lipoxins and aspirin-triggered lipoxins in resolution of inflammation. *Eur. J. Pharmacol.*, 760, 49-63.

[10] Farid, N. A., Kurihara, A., Wrighton, S. A. (2010). Metabolism and disposition of the thienopyridine antiplatelet drugs ticlopidine, clopidogrel, and prasugrel in humans. *J. Clin. Pharmacol.*, 50, 126-142.

[11] Endo, A. A. (2010). Historical perspective on the discovery of statins. *Proc. Jpn. Acad. B: Phys. Biol. Sci.*, 86(5), 484-493.

[12] Carta, F., Innocenti, A., Hall, R. A., Muhlschlegel, F. A., Scozzafava, A., Supuran, C. T. (2011). Carbonic anhydrase inhibitors. Inhibition of the beta-class enzymes from the fungal pathogens Candida albicans and Cryptococcus neoformans with branched aliphatic/aromatic carboxylates and their derivatives. *Bioorg. Med. Chem. Lett.*, 21(8), 2521-2526.

[13] Carta, F., Vullo, D., Maresca, A., Scozzafava, A., Supuran, C. T. (2013). Mono-/dihydroxybenzoic acid esters and phenol pyridinium derivatives as inhibitors of the mammalian carbonic anhydrase isoforms I, II, VII, IX, XII and XIV. *Bioorg. Med. Chem.*, 21(6), 1564-1569.

[14] Supuran, C. T, Capasso, C. (2017). An Overview of the Bacterial Carbonic Anhydrases. *Metabolites*, 7(4), 56.

[15] Tamang, S. R., Cozzolino, A. F., Findlater, M. (2019). Iron catalysed selective reduction of esters to alcohols. *Org. Biomol. Chem.*, 17(7), 1834-8.

[16] Yoshida, M., Hirahata, R., Inoue, T., Shimbayashi, T., Fujita, K. I. (2019). Iridium-catalyzed transfer hydrogenation of ketones and aldehydes using glucose as a sustainable hydrogen donor. *Catalysts*., 9(6), 503.

[17] Mojtahedi, M. M., Samadian, S. (2013). Efficient and rapid solvent-free acetylation of alcohols, phenols, and thiols using catalytic amounts of sodium acetate trihydrate. *J. Chem.*, 2013.

[18] Cronk, J. D., Endrizzi, J. A., Cronk, M. R., O'Neill, J. W., Zhang, K. Y. (2001). Crystal structure of E. coli beta-carbonic anhydrase, an enzyme with an unusual pH-dependent activity. *Protein Sci.*, 10(5), 911-922.

[19] Lu, C., Wu, C., Ghoreishi, D., Chen, W., Wang, L., Damm, W., Dahlgren, M. K., Russell, E., Von Bargen, C. D., Abel, R. (2021). OPLS4: Improving Force Field Accuracy on Challenging Regimes of Chemical Space. *J. Chem. Theory Comput*., 17(7), 4291–300.

[20] Daina, A., Michielin, O., Zoete, V. (2017). SwissADME: a free web tool to evaluate pharmacokinetics, drug-likeness and medicinal chemistry friendliness of small molecules. *Sci. Rep*., 7, 42717.

[21] Daina, A., Michielin, O., Zoete, V. SwissTargetPrediction: updated data and new features for efficient prediction of protein targets of small molecules. Nucleic Acids Res. 2019; 47: W1, W357-W64.

[22] Johnson, M., Zaretskaya, I., Raytselis, Y., Merezhuk, Y., McGinnis, S., Madden, T. L. (2008). NCBI BLAST: a better web interface. *Nucleic Acids Res*., 36: (Web Server issue):W5-9.

[23] Sastry, G. M., Adzhigirey, M., Day, T., Annabhimoju, R., Sherman, W. (2013). Protein and ligand preparation: parameters, protocols, and influence on virtual screening enrichments. *J. Comput. Aided Mol. Des*., 27(3), 221-234.

[24] Friesner, R. A., Murphy, R. B., Repasky, M. P., Frye, L. L., Greenwood, J. R., Halgren, T. A., Sanschagrin, P. C., Mainz, D. T. (2006). Extra precision glide: docking and scoring incorporating a model of hydrophobic enclosure for protein-ligand complexes. *J. Med. Chem*.**,** 49(21), 6177-6196.

[25] Jacobson, M. P., Friesner, R. A., Xiang, Z., Honig, B. (2002). On the role of the crystal environment in determining protein side-chain conformations. *J. Mol. Biol*., 320(3), 597-608.

[26] Lipinski, C. A., Lombardo, F., Dominy, B. W., Feeney, P. J. (2012). Experimental and computational approaches to estimate solubility and permeability in drug discovery and development settings. *Adv. Drug Deliv. Rev.*, 64, 4-17.

[27] Veber, D. F., Johnson, S. R., Cheng, H. Y., Smith, B. R., Ward, K. W., Kopple, K. D. (2002). Molecular properties that influence the oral bioavailability of drug candidates. *J. Med. Chem.*, 45(12), 2615-2623.

[28] Ghose, A. K., Viswanadhan, V. N., Wendoloski, J. J. (1999). A knowledge-based approach in designing combinatorial or medicinal chemistry libraries for drug discovery. 1. A qualitative and quantitative characterization of known drug databases. *J. Comb. Chem*., 1(1), 55-68.

[29] Dvorak, Z. (2011). Drug-drug interactions by azole antifungals: Beyond a dogma of CYP3A4 enzyme activity inhibition. *Toxicol. Lett.*, 202(2), 129-132.

[30] Glaeser, H. Importance of P-glycoprotein for Drug–Drug Interactions. In: Fromm, M., Kim, R. (eds) Drug Transporters. Handbook of Experimental Pharmacology, vol 201. Springer, Berlin, Heidelberg, 2011.

[31] Baell, J., Walters, M. A. (2014). Chemistry: Chemical con artists foil drug discovery. *Nature*, 513(7519), 481-483.

[32] Kimber, M. S., Pai, E. F. (2000). The active site architecture of Pisum sativum beta-carbonic anhydrase is a mirror image of that of alpha-carbonic anhydrases. *EMBO J*., 19(7), 1407-1418.

[33] Mitsuhashi, S., Mizushima, T., Yamashita, E., Yamamoto, M., Kumasaka, T., Moriyama, H., Ueki, T., Miyachi, S., Tsukihara, T. (2000). X-ray structure of beta-carbonic anhydrase from the red alga, Porphyridium purpureum, reveals a novel catalytic site for CO(2) hydration. *J. Biol. Chem*., 275(8), 5521-5526.